

First Application of Mass Measurements with the Rare-RI Ring Reveals the Solar r -Process Abundance Trend at $A = 122$ and $A = 123$

H. F. Li,^{1,2,3,4} S. Naimi,^{3,*} T. M. Sprouse,⁵ M. R. Mumpower,⁵ Y. Abe,³ Y. Yamaguchi,³ D. Nagae,^{3,†} F. Suzaki,^{3,‡} M. Wakasugi,³ H. Arakawa,⁶ W. B. Dou,⁶ D. Hamakawa,⁶ S. Hosoi,⁶ Y. Inada,⁶ D. Kajiki,⁶ T. Kobayashi,⁶ M. Sakaue,⁶ Y. Yokoda,⁶ T. Yamaguchi,⁶ R. Kagesawa,⁷ D. Kamioka,⁷ T. Moriguchi,⁷ M. Mukai,^{7,§} A. Ozawa,⁷ S. Ota,^{8,||} N. Kitamura,⁸ S. Masuoka,⁸ S. Michimasa,⁸ H. Baba,³ N. Fukuda,³ Y. Shimizu,³ H. Suzuki,³ H. Takeda,³ D. S. Ahn,^{3,9} M. Wang,¹ C. Y. Fu,¹ Q. Wang,¹ S. Suzuki,¹ Z. Ge,^{1,¶} Yu. A. Litvinov,¹⁰ G. Lorusso,^{11,12} P. M. Walker,¹² Zs. Podolyak,¹² and T. Uesaka³

¹Institute of Modern Physics, Chinese Academy of Sciences, Lanzhou 730000, People's Republic of China

²Lanzhou University, Lanzhou 730000, People's Republic of China

³Riken Nishina Center for Accelerator-Based Science, Wako, Saitama 351-0198, Japan

⁴University of Chinese Academy of Sciences, Beijing 100049, People's Republic of China

⁵Theoretical Division, Los Alamos National Laboratory, Los Alamos, New Mexico 87545, USA

⁶Department of Physics, Saitama University, Saitama 338-8570, Japan

⁷Institute of Physics, University of Tsukuba, Ibaraki 305-8571, Japan


⁸Center for Nuclear Study, University of Tokyo, Wako, Saitama 351-0198, Japan

⁹Center for Exotic Nuclear Studies, Institute for Basic Science (IBS), Daejeon 34126, Republic of Korea

¹⁰GSI Helmholtzzentrum für Schwerionenforschung, Planckstraße 1, 64291 Darmstadt, Germany

¹¹National Physical Laboratory, Teddington, TW11 0LW, United Kingdom

¹²Department of Physics, University of Surrey, Guildford GU2 7XH, United Kingdom

 (Received 9 December 2021; revised 31 January 2022; accepted 15 February 2022; published 15 April 2022)

The Rare-RI Ring (R3) is a recently commissioned cyclotronlike storage ring mass spectrometer dedicated to mass measurements of exotic nuclei far from stability at Radioactive Isotope Beam Factory (RIBF) in RIKEN. The first application of mass measurement using the R3 mass spectrometer at RIBF is reported. Rare isotopes produced at RIBF— ^{127}Sn , ^{126}In , ^{125}Cd , ^{124}Ag , ^{123}Pd —were injected in R3. Masses of ^{126}In , ^{125}Cd , and ^{123}Pd were measured whereby the mass uncertainty of ^{123}Pd was improved. This is the first reported measurement with a new storage ring mass spectrometry technique realized at a heavy-ion cyclotron and employing individual injection of the preidentified rare nuclei. The latter is essential for the future mass measurements of the rarest isotopes produced at RIBF. The impact of the new ^{123}Pd result on the solar r -process abundances in a neutron star merger event is investigated by performing reaction network calculations of 20 trajectories with varying electron fraction Y_e . It is found that the neutron capture cross section on ^{123}Pd increases by a factor of 2.2 and β -delayed neutron emission probability, P_{1n} , of ^{123}Rh increases by 14%. The neutron capture cross section on ^{122}Pd decreases by a factor of 2.6 leading to pileup of material at $A = 122$, thus reproducing the trend of the solar r -process abundances. The trend of the two-neutron separation energies (S_{2n}) was investigated for the Pd isotopic chain. The new mass measurement with improved uncertainty excludes large changes of the S_{2n} value at $N = 77$. Such large increase of the S_{2n} values before $N = 82$ was proposed as an alternative to the quenching of the $N = 82$ shell gap to reproduce r -process abundances in the mass region of $A = 112$ –124.

DOI: 10.1103/PhysRevLett.128.152701

The discovery of the historical GW170817 event of binary neutron stars merger and the subsequent kilonova AT2017go [1] for the GW170817 [2] was a major milestone toward revealing the secret of the synthesis of heavy elements via the rapid neutron capture process (r -process) [3]. The recent identification of strontium in the kilonova radiation gave a strong evidence of the production of r -process elements [4]. However, modeling of the accretion disk formed in supernova-triggered collapse of rapidly rotating massive stars, or collapsars, showed that r -process elements could be also produced in considerable

amounts [5]. The presence of r -process heavy elements was also observed in the dwarf galaxy Reticulum II [6], where the accretion disk of collapsars might be the main source of production. Heavy elements might be therefore synthesized in various astrophysical sites such as neutron star mergers and magnetorotational supernovas [7,8]. To model the formation of heavy chemical elements under different astrophysical conditions, a large and diverse amount of nuclear data is needed, especially for neutron-rich nuclei that live for a fraction of a second. Nuclear masses are important ingredients since they reflect the neutron

separation energies, which are required for the determination of neutron capture and photodissociation rates [3,9,10]. A vast number of neutron-rich nuclei involved in the r -process can now be produced in the laboratory at rare isotope facilities and their properties measured with high precision. However, all nuclei needed for modeling the r -process will not be accessible even at the new-generation radioactive-ion beam facilities. A robust model based on accurate properties of neutron-rich nuclei is thus essential to reveal the astrophysical conditions in which heavy elements could be produced. Such a model will help quantify the production rates in various sites, which will result in more accurate nucleosynthesis calculations capable of reproducing the r -process elements' chemical abundances [11,12].

This Letter reports precision mass measurements of neutron-rich nuclei produced at the Radioactive Isotope Beam Factory (RIBF) and their implication in the production of r -process elements with atomic mass number $A = 122$ and $A = 123$. Mass measurements of nuclei with neutron number $N = 77$ were performed for the first time with a new type of mass spectrometer, namely the Rare-RI Ring (R3), recently commissioned at the RIKEN RIBF facility [13]. We examine the implication of the ^{123}Pd mass on the abundance calculation for conditions representing a neutron star merger event. These first mass measurements at RIBF of neutron-rich isotopes in a remote region of the nuclear chart open a door to reaching r -process nuclei at $N = 82$ and beyond.

In the experiment, the secondary beam was produced by in-flight fission of the 345 MeV/nucleon ^{238}U beam provided by the Superconducting Ring Cyclotron impinged on the 6-mm thick beryllium target that was placed upstream of the BigRIPS separator at F0 focal plane (see Fig. 1). The secondary fragments of interest were separated by the first stage of the BigRIPS as described in [14]. For this purpose, a 5-mm wedge-shaped degrader was introduced at the F1 focal plane of the BigRIPS. The magnetic rigidity $B\rho$ and the transmission efficiency were optimized for the reference particle ^{124}Ag . The momentum selection was done by setting the slits at F1 to ± 2 mm, corresponding to the R3 momentum acceptance of $\pm 0.3\%$. The injection kicker magnets system placed inside the R3 is limited to a repetition rate of 100 Hz. Therefore, to accept the quasicontinuous beam from the Superconducting Ring Cyclotron, the individual self-triggered injection technique was developed for injecting preidentified particles of interest [15]. The particle identification was achieved by the ΔE -TOF method in the beam line, where ΔE is the energy loss measured by the ionization chamber (IC) placed at F3 and TOF is the time-of-flight measured by the plastic scintillator at F3 and the E-MCP detector [16] at S0 of the SHARAQ spectrometer. Also a 2-mm thick plastic scintillator was placed after the IC at F3 to get a rough ΔE information needed for removing contaminants [17]. Two parallel plate avalanche counter (PPAC) position monitors were installed at F3 to monitor the beam size and two double PPACs were installed at F5, which is a

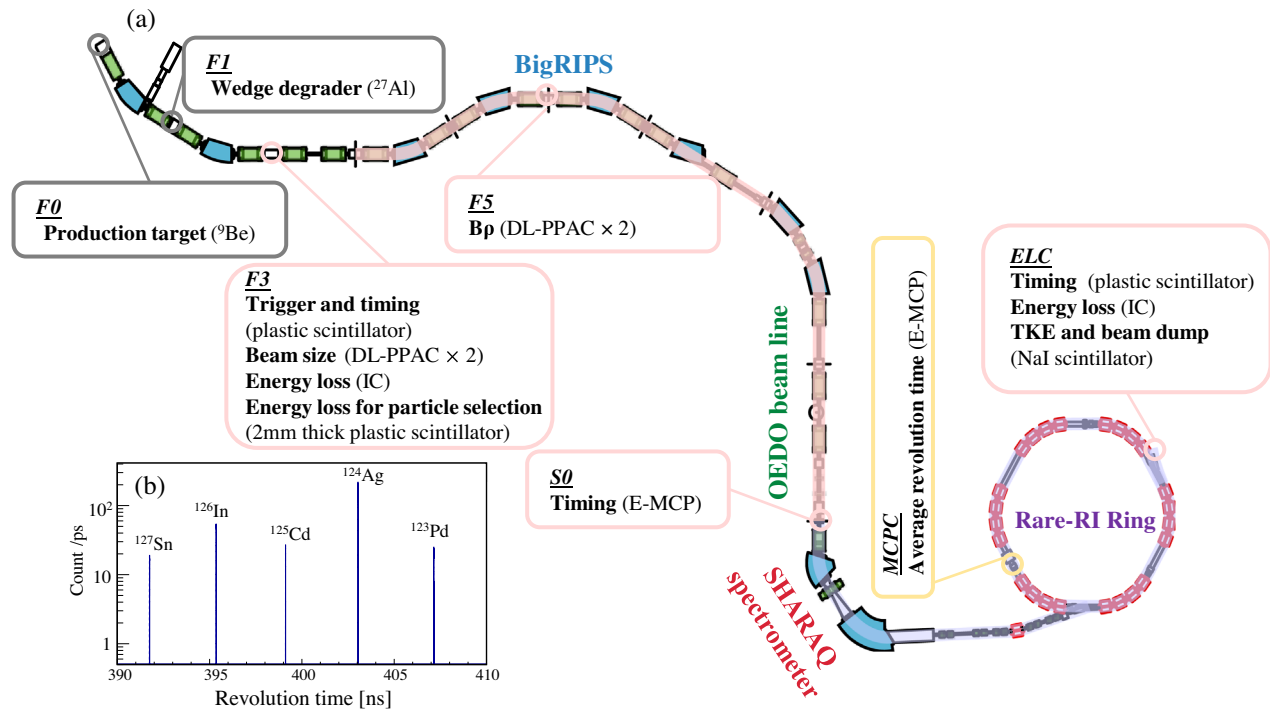


FIG. 1. (a) Configuration of the detectors installed in the beam line and Rare-RI Ring (R3). (b) The revolution time spectrum for the nuclei measured in this work. The background free spectrum reflects the efficiency of event-by-event tracking.

dispersive focal plane to measure $B\rho$ of every individual particle prior to its injection into the R3. The particle circulated in the R3 for about 1800 revolutions before it was ejected from the ring. The total TOF in the R3 was measured by the E-MCP detector at S0 and a plastic scintillator detector placed at extraction line chamber (ELC) after the ejection from the R3. Another IC was installed at ELC, where an additional particle identification was performed. Finally, particles were stopped in the NaI scintillator detector placed behind the IC at ELC.

The mass-to-charge ratio (m/q) of the particle of interest with a revolution time T is determined relative to a reference particle with m_0/q_0 and T_0 by using the following formula [13,18]:

$$\frac{m}{q} = \frac{m_0}{q_0} \frac{T}{T_0} \sqrt{\frac{1 - \beta^2}{1 - (\frac{T}{T_0}\beta)^2}} \quad (1)$$

where β is the velocity of the particle of interest relative to the speed of light in vacuum. Revolution time spectrum of all injected nuclei is shown in Fig. 1(b) (details of determination of the revolution time in R3 can be found in [19]). Since the isochronous condition of the ring is optimized for the reference particle, T_0 is independent of the momentum. To determine the mass, the velocity β needs to be determined event-by-event from the time-of-flight along the beamline from F3 to S0 ($\text{TOF}_{3,50}$) by using the following equation:

$$\beta = \frac{\text{Length}_{3,50}}{(\text{TOF}_{3,50} + \text{TOF}_{\text{offset}})}. \quad (2)$$

The average path length from F3 to S0 ($\text{Length}_{3,50}$) and the $\text{TOF}_{\text{offset}}$ caused by the electronics and the energy loss in the detectors on the beamline, are determined via Eq. (2) by using known masses of ^{124}Ag and ^{127}Sn . The parameters that could reproduce the known m/q values are $\text{Length}_{3,50} = 84.859(2)$ m and $\text{TOF}_{\text{offset}} = 325.47(1)$ ns. The mass is then determined for each event via Eq. (1). Additional systematic uncertainties, σ_{sys} , due to the determination of parameters such as $\text{Length}_{3,50}$, $\text{TOF}_{\text{offset}}$ and T_0 were estimated and reported in Table I. Details of data analysis method can be found in Refs. [13,19]. The full data analysis method as well as the details of estimating the systematic uncertainties will be reported in a subsequent

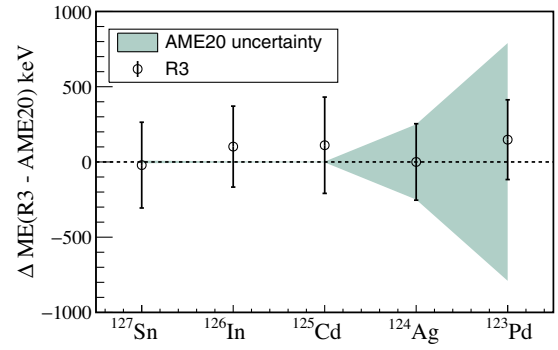


FIG. 2. Mass excess values of nuclei measured at R3 compared to literature values from AME2020 [20].

publication. The determined mass excess values are listed in Table I. Comparison with literature values from the latest Atomic Mass Evaluation, AME2020 [20], are plotted in Fig. 2. As shown in Table I, the uncertainties are dominated by the mass uncertainty of the reference particle ^{124}Ag . The choice of this reference instead of ^{125}Cd , which has lower uncertainty, is mainly due to the presence of a long-lived isomeric state at 186 keV in the latter that is difficult to separate with R3. The mass precision was therefore sacrificed for higher accuracy. However, if the mass of ^{124}Ag is remeasured with higher precision, the uncertainties of all other masses will be reduced.

Subtle nuclear structure effects of neutron-rich nuclei are believed to have strong impact on the r -process abundances [21,22]. Failure to produce enough material for masses at $A = 112\text{--}124$ was thought to be due to the shell quenching at $N = 82$ [23]. However, it has been recently demonstrated through mass measurement of ^{132}Cd that this shell gap, although reduced, is not quenched for $Z < 50$ [24]. Another suggested solution to this issue was the increase of the two-neutron separation energies (S_{2n}) that might be associated with a sudden transition from deformed shape to spherical shape for nuclei with $Z < 50$ and $N = 75\text{--}82$ [21]. In Fig. 3, the S_{2n} values for Cd and Pd isotopic chains are shown with the updated value for the most neutron-rich Pd isotope at $N = 77$. Global mass models (FRDM [25], KTUY05 [26], EFTSI-Q [27], and WS4 + RBF [28]) are also plotted in addition to the microscopic mass model HFB24 [29] and its more recent version HFB31 [30]. Changes in the S_{2n} values of the most recent mass models are significantly less pronounced for Pd isotopes as

TABLE I. Mass excess values from literature and measured in this work are shown in the second and third column, respectively. Total uncertainties are shown as well as the contribution from the reference mass uncertainty σ_{m_0} and the statistical uncertainty σ_{stat} . The systematic uncertainty σ_{sys} is estimated from the uncertainty of T_0 and the fit parameters $\text{Length}_{3,50}$ and $\text{TOF}_{\text{offset}}$ in Eq. (2).

Nucleus	ME _{AME20} (keV)	ME _{R3} (keV)	σ_{total} (keV)	σ_{m_0} (keV)	σ_{stat} (keV)	σ_{sys} (keV)
^{126}In	-77 809(4)	-77 707	269	254	65	62
^{125}Cd	-73 348.1(29)	-73 237	320	252	192	40
^{123}Pd	-60 430(790)	-60 282	265	248	86	40

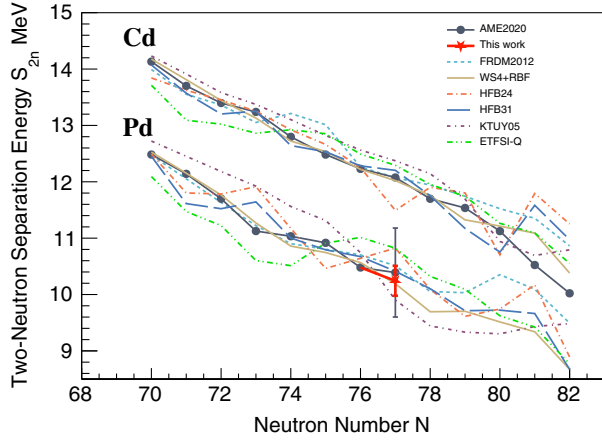


FIG. 3. The two-neutron separation energy values (S_{2n}) for Cd and Pd isotopic chains. Experimental data are taken from AME2020 [20]. The S_{2n} value derived from our new mass value of ^{123}Pd is shown in red, while the theoretical predictions are shown by the colored dash lines [25–30].

compared to earlier mass models such as ETFSI-Q, KTUY05, and HFB24. The new S_{2n} value of ^{123}Pd shows a smooth decrease following the trend of the mass surface. Furthermore, the improvement of the uncertainty excludes significant large change in the S_{2n} value at $N = 77$ as compared to the uncertainty of the ^{123}Pd mass reported in the AME2020.

We simulate the impact of the mass measurement of ^{123}Pd in the r -process by employing the Portable Routines for Integrated nucleoSynthesis Modeling reaction network [31,32]. The baseline nuclear physics properties are simulated with FRDM2012 [25,33–36]. The mass of ^{123}Pd in the baseline model is also taken from the FRDM2012. Changes to the mass propagate to cross sections and branching ratios in neighboring nuclei as in Ref. [10]. We find that the changes in the capture cross sections and β -delayed neutron probabilities (discussed below) have a significant effect as compared with propagation to separation energies alone. Past studies have indicated that the mass of ^{123}Pd is most influential for abundances of nearby isobars [37], in particular the abundances of $A = 122$ and $A = 123$, so we analyze the impact of the measured mass from this perspective.

Since there are uncertainties in the astrophysical conditions that could produce nuclei in the mass $A \sim 120$ range, we simulate nucleosynthesis for a set of 20 parameterized r -process trajectories [38] with specific entropy $40 k_B/\text{baryon}$, timescale $\tau = 20$ ms, and electron fraction running from $Y_e = 0.15$ to $Y_e = 0.35$ in intervals of 0.01. Figure 4 shows the change in the $A = 122$ to $A = 123$ abundance ratio for each trajectory due to the ^{123}Pd mass measurement when compared against the baseline model. For all trajectories considered here, the overall effect is the increase of the ratio with respect to the baseline, with the largest effects noted for the lowest electron fractions

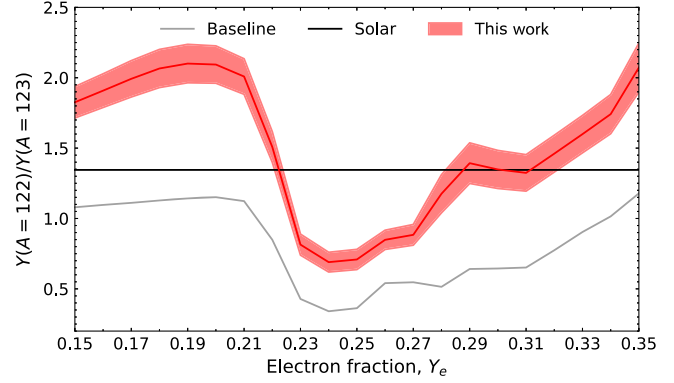


FIG. 4. Ratio of the $A = 122$ to $A = 123$ isotopic abundances as a function of electron fraction for the baseline model (gray line) and if our new mass measurement (red line) and its uncertainty (red band) are included. The horizontal black line indicates the value of the same ratio in the solar r -process residuals of Ref. [39].

considered, $Y_e < 0.22$. In all of these trajectories, the baseline model fails to achieve the solar ratio, such that no combination of these trajectories would be able to reproduce this observed feature. However, when we update the nuclear data to include the measured ^{123}Pd mass, the ratio is sufficiently varied across the range of trajectories, such that suitable linear combinations of these make reproduction of this ratio a viable possibility. This can be achieved, for example, by mixing contributions from trajectories that overproduce or underproduce $A = 122$ nuclei relative to $A = 123$ nuclei. The effect arises due to changes in calculated nuclear properties introduced by the newly measured ^{123}Pd mass. The neutron capture cross section for ^{122}Pd decreases by a factor of 2.6 and for ^{123}Pd increases by a factor of 2.2, while the P_{1n} value, probability for the β -delayed neutron emission, of ^{123}Rh increases by 14% with the updated mass. This results in an effective pileup of material along the $A = 122$ isobar relative to the baseline. We note that sizeable statistical model uncertainties exist in the γ -strength function and level density of neutron-rich nuclei; here we consider the impact of the current measurement in isolation to other uncertainties.

In summary, the first implementation of mass measurements performed by the Rare-RI Ring at the RIBF facility is reported. The most neutron-rich nuclei below the doubly magic nucleus ^{132}Sn were studied, opening a new avenue to perform mass measurements of r -process nuclei near $N = 82$. To reproduce the r -process abundances with masses $A = 112$ – 124 , an increase of S_{2n} values just before the $N = 82$ for neutron-rich nuclei with $Z < 50$ was proposed as an alternative to $N = 82$ shell gap quenching. The new mass measurement of ^{123}Pd and its uncertainty exclude large change of the S_{2n} value at $N = 77$ for the Pd isotopic chain. We performed calculations to estimate the impact of the ^{123}Pd mass measured in the r -process. We found that if our new mass value is used instead of the

FRDM value, the r -process abundances at $A = 122$ and $A = 123$ are modified toward being more consistent with solar values. This indicates that the r -process calculations are very sensitive to masses in this region since a change of ^{123}Pd mass by just 478 keV causes a sizeable effect. This finding highlights the need for high precision mass measurements to address the r -process in this mass region.

We are grateful to the RIKEN RIBF accelerator crew and CNS, University of Tokyo, for their efforts and support to operate the RI beam factory. H. F. L. expresses gratitude to the RIKEN International Program Associate. This work was supported by the RIKEN Pioneering Project Funding (“Extreme precisions to Explore fundamental physics with Exotic particles”) and JSPS KAKENHI Grants No. 19K03901, 26287036, 25105506, 15H00830, 17H01123, 18H03695, 17K14311. T. M. S. and M. R. M. were supported by the US Department of Energy through the Los Alamos National Laboratory (LANL). LANL is operated by Triad National Security, LLC, for the National Nuclear Security Administration of U.S. Department of Energy (Contract No. 89233218CNA000001). T. M. S. was partly supported by the Fission In R-process Elements (FIRE) Topical Collaboration in Nuclear Theory, funded by the U.S. Department of Energy. Y. A. L. acknowledges support by the European Research Council (ERC) under the European Union’s Horizon 2020 research and innovation program (Grant Agreement No. 682841 “ASTRUM”). This work is supported by the UK Science and Technology Facilities Council under Grant No. ST/P005314/1 and the National Natural Science Foundation of China (Grant No. 11975280).

*Corresponding author.
snaimi@ribf.riken.jp

[†]Present address: Research Center for SuperHeavy Elements, Kyushu University, Fukuoka, Fukuoka 819-0395, Japan.

[‡]Present address: Advanced Science Research Center, Japan Atomic Energy Agency, Ibaraki 319-1195, Japan.

[§]Present address: Riken Nishina Center for Accelerator-Based Science, Wako, Saitama 351-0198, Japan.

^{||}Present address: Research Center for Nuclear Physics, Osaka University, Osaka 567-0047, Japan.

[¶]Present address: GSI Helmholtzzentrum für Schwerionenforschung, Planckstraße 1, 64291 Darmstadt, Germany.

- [1] B. P. Abbott *et al.*, Multi-messenger observations of a binary neutron star merger, *Astrophys. J.* **848**, L12 (2017).
- [2] B. P. Abbott, R. Abbott, T. Abbott, F. Acernese, K. Ackley, C. Adams, T. Adams, P. Addesso, R. Adhikari, V. Adya *et al.*, Gw170817: Observation of Gravitational Waves from a Binary Neutron Star Inspiral, *Phys. Rev. Lett.* **119**, 161101 (2017).
- [3] E. M. Burbidge, G. R. Burbidge, W. A. Fowler, and F. Hoyle, Synthesis of the elements in stars, *Rev. Mod. Phys.* **29**, 547 (1957).
- [4] D. Watson, C. J. Hansen, J. Selsing, A. Koch, D. B. Malesani, A. C. Andersen, J. P. Fynbo, A. Arcones, A. Bauswein, S. Covino *et al.*, Identification of strontium in the merger of two neutron stars, *Nature (London)* **574**, 497 (2019).
- [5] D. M. Siegel, J. Barnes, and B. D. Metzger, Collapsars as a major source of r-process elements, *Nature (London)* **569**, 241 (2019).
- [6] A. P. Ji, A. Frebel, A. Chiti, and J. D. Simon, R-process enrichment from a single event in an ancient dwarf galaxy, *Nature (London)* **531**, 610 (2016).
- [7] J. J. Cowan, C. Sneden, J. E. Lawler, A. Aprahamian, M. Wiescher, K. Langanke, G. Martínez-Pinedo, and F.-K. Thielemann, Origin of the heaviest elements: The rapid neutron-capture process, *Rev. Mod. Phys.* **93**, 015002 (2021).
- [8] C. J. Horowitz *et al.*, r-process nucleosynthesis: Connecting rare-isotope beam facilities with the cosmos, *J. Phys. G* **46**, 083001 (2019).
- [9] R. Surman, J. Beun, G. C. McLaughlin, and W. R. Hix, Neutron capture rates near $A = 130$ that effect a global change to the r -process abundance distribution, *Phys. Rev. C* **79**, 045809 (2009).
- [10] M. R. Mumpower, R. Surman, D. L. Fang, M. Beard, P. Möller, T. Kawano, and A. Aprahamian, Impact of individual nuclear masses on r-process abundances, *Phys. Rev. C* **92**, 035807 (2015).
- [11] B. Côté, K. Belczynski, C. L. Fryer, C. Ritter, A. Paul, B. Wehmeyer, and B. W. O’Shea, Advanced LIGO constraints on neutron star mergers and r-process sites, *Astrophys. J.* **836**, 230 (2017).
- [12] K. Hotokezaka, P. Beniamini, and T. Piran, Neutron star mergers as sites of r-process nucleosynthesis and short gamma-ray bursts, *Int. J. Mod. Phys. D* **27**, 1842005 (2018).
- [13] D. Nagae, S. Omika, Y. Abe, Y. Yamaguchi, F. Suzaki, K. Wakayama, N. Tadano, R. Igosawa, K. Inomata, H. Arakawa *et al.*, First demonstration of mass measurements for exotic nuclei using rare-RI ring, in *Proceedings of 10th International Conference on Nuclear Physics at Storage Rings (STORI’17)* (Physical Society of Japan, Kanazawa, 2021), p. 011014, [10.7566/JPSCP.35.011014](https://doi.org/10.7566/JPSCP.35.011014).
- [14] N. Fukuda, T. Kubo, T. Ohnishi, N. Inabe, H. Takeda, D. Kameda, and H. Suzuki, Identification and separation of radioactive isotope beams by the bigrips separator at the riken RI beam factory, *Nucl. Instrum. Methods Phys. Res., Sect. B* **317**, 323 (2013), xVIth International Conference on ElectroMagnetic Isotope Separators and Techniques Related to their Applications, December 2–7, 2012 at Matsue, Japan.
- [15] Y. Yamaguchi, Y. Abe, F. Suzaki, M. Wakasugi, and Rare-RI Ring collaborators, Commissioning of the Rare-RI Ring at RIKEN RI Beam Factory, FRYAUD01 (2021), <https://accelconf.web.cern.ch/cool2015/papers/proceed.pdf>.
- [16] D. Nagae, Y. Abe, S. Okada *et al.*, Development and operation of an electrostatic time-of-flight detector for the rare RI storage ring, *Nucl. Instrum. Methods Phys. Res., Sect. A* **986**, 164713 (2021).
- [17] A. Abe, Y. Yamaguchi, M. Wakasugi, D. Nagae, F. Suzuki, and for the Rare RI Ring Collaboration, Update of the particle selection system for the rare RI ring experiments, RIKEN Accel. Prog. Rep. **52**, 15 (2019), <https://www.nishina.riken.jp/researcher/APR/APR052/pdf/15.pdf>.

- [18] A. Ozawa, T. Uesaka, M. Wakasugi, and the Rare-RI Ring Collaboration, The rare-RI ring, *Prog. Theor. Exp. Phys.* **2012** (2012), 03C009.
- [19] S. Naimi, H. Li, Y. Abe *et al.*, Experimental challenges of the first mass measurement campaign at the rare-RI ring, *J. Phys.* **1643**, 012058 (2020).
- [20] M. Wang, W. Huang, F. Kondev, G. Audi, and S. Naimi, The AME 2020 Atomic Mass Evaluation (II) tables, graphs and references, *Chin. Phys. C* **45**, 030003 (2021).
- [21] H. Grawe, K. Langanke, and G. Martínez-Pinedo, Nuclear structure and astrophysics, *Rep. Prog. Phys.* **70**, 1525 (2007).
- [22] A. Arcones and G. Martínez-Pinedo, Dynamical r -process studies within the neutrino-driven wind scenario and its sensitivity to the nuclear physics input, *Phys. Rev. C* **83**, 045809 (2011).
- [23] J. Pearson, R. Nayak, and S. Goriely, Nuclear mass formula with bogolyubov-enhanced shell-quenching: Application to r -process, *Phys. Lett. B* **387**, 455 (1996).
- [24] V. Manea, J. Kartheim, D. Atanasov, M. Bender, K. Blaum, T. E. Cocolios, S. Eliseev, A. Herlert, J. D. Holt, W. J. Huang, Y. A. Litvinov, D. Lunney, J. Menéndez, M. Mougeot, D. Neidherr, L. Schweikhard, A. Schwenk, J. Simonis, A. Welker, F. Wienholtz, and K. Zuber, First Glimpse of the $N = 82$ Shell Closure Below $Z = 50$ from Masses of Neutron-Rich Cadmium Isotopes and Isomers, *Phys. Rev. Lett.* **124**, 092502 (2020).
- [25] P. Möller, A. J. Sierk, T. Ichikawa, and H. Sagawa, Nuclear ground-state masses and deformations: FRDM(2012), *At. Data Nucl. Data Tables* **109**, 1 (2016).
- [26] H. Koura, T. Tachibana, M. Uno, and M. Yamada, Nuclidic mass formula on a spherical basis with an improved even-odd term, *Prog. Theor. Phys.* **113**, 305 (2005).
- [27] J. Pearson, R. Nayak, and S. Goriely, Nuclear mass formula with bogolyubov-enhanced shell-quenching: Application to r -process, *Phys. Lett. B* **387**, 455 (1996).
- [28] N. Wang, M. Liu, X. Wu, and J. Meng, Surface diffuseness correction in global mass formula, *Phys. Lett. B* **734**, 215 (2014).
- [29] S. Goriely, N. Chamel, and J. M. Pearson, Further explorations of skyrme-hartree-fock-bogoliubov mass formulas. xiii. the 2012 atomic mass evaluation and the symmetry coefficient, *Phys. Rev. C* **88**, 024308 (2013).
- [30] S. Goriely, N. Chamel, and J. M. Pearson, Further explorations of skyrme-hartree-fock-bogoliubov mass formulas. xvi. inclusion of self-energy effects in pairing, *Phys. Rev. C* **93**, 034337 (2016).
- [31] T. M. Sprouse, R. Navarro Perez, R. Surman, M. R. Mumpower, G. C. McLaughlin, and N. Schunck, Propagation of statistical uncertainties of Skyrme mass models to simulations of r -process nucleosynthesis, *Phys. Rev. C* **101**, 055803 (2020).
- [32] T. M. Sprouse, M. R. Mumpower, and R. Surman, Following nuclei through nucleosynthesis: A novel tracing technique, *Phys. Rev. C* **104**, 015803 (2021).
- [33] P. Möller, A. J. Sierk, T. Ichikawa, A. Iwamoto, and M. Mumpower, Fission barriers at the end of the chart of the nuclides, *Phys. Rev. C* **91**, 024310 (2015).
- [34] M. R. Mumpower, T. Kawano, and P. Möller, Neutron- γ competition for β -delayed neutron emission, *Phys. Rev. C* **94**, 064317 (2016).
- [35] M. R. Mumpower, T. Kawano, T. M. Sprouse, N. Vassh, E. M. Holmbeck, R. Surman, and P. Möller, β -delayed fission in r -process nucleosynthesis, *Astrophys. J.* **869**, 14 (2018).
- [36] P. Möller, M. R. Mumpower, T. Kawano, and W. D. Myers, Nuclear properties for astrophysical and radioactive-ion-beam applications (II), *At. Data Nucl. Data Tables* **125**, 1 (2019).
- [37] M. R. Mumpower, R. Surman, G. C. McLaughlin, and A. Aprahamian, The impact of individual nuclear properties on r -process nucleosynthesis, *Prog. Part. Nucl. Phys.* **86**, 86 (2016).
- [38] Y. Zhu, R. T. Wollaeger, N. Vassh, R. Surman, T. M. Sprouse, M. R. Mumpower, P. Möller, G. C. McLaughlin, O. Korobkin, T. Kawano, P. J. Jaffke, E. M. Holmbeck, C. L. Fryer, W. P. Even, A. J. Couture, and J. Barnes, Californium-254 and kilonova light curves, *Astrophys. J.* **863**, L23 (2018).
- [39] M. Arnould, S. Goriely, and K. Takahashi, The r -process of stellar nucleosynthesis: Astrophysics and nuclear physics achievements and mysteries, *Phys. Rep.* **450**, 97 (2007).